New PAPR-Preserving Mapping Methods for Single-Carrier FDMA with Space-Frequency Block Codes

Cristina Ciochina, Damien Castelain, David Mottier, and Hikmet Sari, *Fellow, IEEE*

***Abstract*—Innovative mapping schemes for Space-Frequency Block Codes (SFBC) which are compatible with the structure of Single-Carrier Frequency Division Multiple Access (SC-FDMA) systems are introduced. We first show that existing space-time and space-frequency block codes lack flexibility in terms of framing or cause a degradation of the signal envelope properties when combined with SC-FDMA. Then, we present an Alamouti-based orthogonal code designed for 2 transmit antennas that makes use of an innovative mapping in the frequency domain to preserve the low envelope properties of SC-FDMA. Next, an extension of this concept to a quasi-orthogonal code for 4 transmit antennas is presented and analyzed. We prove the good performance of the proposed schemes over multiple-input multiple-output (MIMO) channels both in static and in high-mobility scenarios.**

***Index Terms*—Space-Frequency Block Code (SFBC), Space-Time Block Code (STBC), Single-Carrier Frequency Division Multiple Access (SC-FDMA), Peak-to-Average Power Ratio (PAPR), Multiple-Input Multiple-Output (MIMO).**

I. Introduction

MULTIPLE-Input Multiple-Output (MIMO) techniques have become an indispensable part of wireless communications systems in order to satisfy the ever increasing demands for higher throughput or improved performance. The use of multiple antennas both at the base station and at the terminal can improve the bit error rate (BER) performance by benefiting from spatial diversity, increase the transmitted data rate through spatial multiplexing, reduce interference from other users, or make some trade-off among the above. MIMO techniques have been incorporated in all recent wireless communications standards (e.g., IEEE 802.11n for wireless local area networks - WLAN, IEEE 802.16e-2005 for mobile WiMAX, etc.) [1], most of them relying on OFDMA (Orthogonal Frequency Division Multiple Access) or one of its derivatives. This multi-carrier (MC) radio access is very popular for its well-known advantages: Good spectral efficiency, good coverage, flexible dynamic frequency allocation, simple equalization at tone level [2], etc. But OFDMA has the drawback of high peak-to-average power ratio (PAPR), which is a common characteristic of all MC modulations [3]. Significant efforts are being made to efficiently reduce the PAPR [4].

For the uplink of Long Term Evolution (LTE) of UMTS (Universal Mobile Telecommunications System), the Third Generation Partnership Project (3GPP) opted for a precoded OFDMA air interface, called Single-Carrier Frequency Division Multiple Access (SC-FDMA). The precoder is a Direct Fourier Transform (DFT), which restores the low envelope fluctuations of SC systems [5]. But SC-FDMA loses this property in MIMO systems if no precaution is taken. Indeed, conventional space-frequency block codes (SFBCs) permute the spectral components of the transmitted signal and destroy the low PAPR property.

In this paper, we present an innovative mapping which preserves the low PAPR property of SC-FDMA with SFBCs. The paper is organized as follows: Conventional transmit diversity schemes in conjunction with SC-FDMA are presented in Section II. Two novel SFBC schemes with innovative mapping are described in Sections III and IV, respectively. Their performance is assessed in Section V, and finally, Section VI gives our conclusions.

II. Space Time and Frequeny Coding in SC-FDMA

In this paper, the notations $(.)^{-1}$, $(.)^{\dagger}$, $(.)^{\mathrm{T}}$, $(.)^{\mathrm{H}}$, $(.)^{*}$ and $\otimes$ stand for the inverse, pseudo-inverse, transpose, Hermitian, complex conjugate and Kronecker product of vectors or matrices, respectively. All signals will be represented by their discrete-time baseband equivalents. We will use the following notations:

- $\mathbf{J} = \begin{bmatrix} 0 & 1 \\ -1 & 0 \end{bmatrix}$, $\mathbf{0}_2 = \begin{bmatrix} 0 & 0 \\ 0 & 0 \end{bmatrix}$;
- $\mathbf{P}_M^{(\mathbf{J})}$ an M-sized block-diagonal matrix containing $M/2$ copies of $\mathbf{J}$ on its main diagonal, and $\bar{\mathbf{P}}_M^{(\mathbf{J})}$ is the M-sized block-antidiagonal matrix containing $M/2$ copies of $\mathbf{J}$ on its secondary diagonal:

$$\mathbf{P}_{\mathbf{M}}^{(\mathbf{J})} = \begin{bmatrix} \begin{bmatrix} 0 & 1 \\ -1 & 0 \end{bmatrix} & \mathbf{0}_2 & \cdots & \mathbf{0}_2 \\ \mathbf{0}_2 & \begin{bmatrix} 0 & 1 \\ -1 & 0 \end{bmatrix} & \cdots & \mathbf{0}_2 \\ \vdots & \vdots & \ddots & \vdots \\ \mathbf{0}_2 & \mathbf{0}_2 & \cdots & \begin{bmatrix} 0 & 1 \\ -1 & 0 \end{bmatrix} \end{bmatrix} \quad (1)$$

Manuscript received September 12, 2008; revised May 22, 2009; accepted June 17, 2009. The associate editor coordinating the review of this paper and approving it for publication was X. Xia.

C. Ciochina, D. Castelain and D. Mottier are with the Wireless CommunicationsSystems Department, Mitsubishi Electric R&D Centre Europe, 1 Allée de Beaulieu, 35708 Rennes, France, e-mail: [c.ciochina,d.castelain,d.mottier@fr.merce.mee.com].

H. Sari is with the Telecommunications Department, École Supérieure d'Électricité, 1-3 Rue Joliot Curie, 91192 Gif sur Yvette, France, e-mail: hikmet.sari@supelec.fr.

$$\bar{\mathbf{P}}_M^{(\mathbf{J})} = \begin{bmatrix} \mathbf{0}_2 & \cdots & \mathbf{0}_2 & \begin{bmatrix} 0 & 1 \\ -1 & 0 \end{bmatrix} \\ \mathbf{0}_2 & \cdots & \begin{bmatrix} 0 & 1 \\ -1 & 0 \end{bmatrix} & \mathbf{0}_2 \\ \vdots & \iddots & \vdots & \vdots \\ \begin{bmatrix} 0 & 1 \\ -1 & 0 \end{bmatrix} & \cdots & \mathbf{0}_2 & \mathbf{0}_2 \end{bmatrix} \tag{2}$$

- $\mathbf{F}_M$ the $M \times M$ matrix describing a normalized M-point DFT, with elements $F_{k,n} = \omega_M^{kn}/\sqrt{M}$ on the *k*-th row and *n*-th column, where $k, n = 0...M-1$ and $\omega_M = \mathrm{e}^{-j2\pi/M}$ is a primitive root of unity;
- $\mathbf{F}_M^{-1} = \mathbf{F}_M^{\mathrm{H}} = \mathbf{F}_M^*$, the M-point inverse DFT (IDFT);
- $\mathbf{S}_M^p$ is an operator which cyclically shifts the rows of an *M*-sized matrix down by *p* positions:

$$\mathbf{S}_M^p = \begin{bmatrix} 0 & \cdots & \cdots & 0 & 1 \\ 1 & 0 & & 0 & 0 \\ 0 & 1 & \ddots & \vdots & \vdots \\ \vdots & \ddots & \ddots & 0 & \vdots \\ 0 & \cdots & 0 & 1 & 0 \end{bmatrix}^p . \tag{3}$$

For any complex vector $\mathbf{x} = [x_0, x_1, x_2, ..., x_{M-1}]^{\mathrm{T}}$ the following properties and inequalities hold:

(P1): $\bar{\mathbf{x}} = \mathbf{F}_M^{\mathrm{H}}\mathbf{F}_M^{\mathrm{H}}\mathbf{x} = [x_0, x_{M-1}, x_{M-2}, ..., x_1]^{\mathrm{T}}$ is the time reversed version of vector $\mathbf{x}$ ($\bar{x}_k = x_{(-k) \bmod M}$, where mod is the modulo operator and $k = 0...M-1$) [6].

(I1): $\left|\sum_{i=0}^{M-1} x_i y_i\right|^2 \leq \left(\sum_{i=0}^{M-1} |x_i|^2\right)\left(\sum_{i=0}^{M-1} |y_i|^2\right)$, where $x_i \in \mathbb{C}$ (the Cauchy-Schwarz inequality [7]). The equality holds if and only if $\mathbf{x}$ and $\mathbf{y}$ are linearly dependent, *i.e.*, one is a scalar multiple of the other.

(I2): $\left|\sum_{i=0}^{M-1} x_i\right| \leq \sum_{i=0}^{M-1} |x_i|$, where $x_i \in \mathbb{C}$. Equality holds if and only if all x_i have the same argument, that is, $x_i = |x_i|\, e^{j\phi_0}, \phi_0 \in [0, 2\pi), \forall i = 0...M-1$.

A. SC-FDMA and Antenna Precoding

As opposed to MC-FDMA schemes, SC-FDMA combines a single-carrier signal with an OFDMA-like multiple access and attempts to achieve the advantages of both techniques: Low PAPR and flexible dynamic frequency allocation. In what follows, we review the principles of SC-FDMA, determine at what point in the transmitter it is possible to implement transmit diversity precoding, and finally, we give a system model for SC-FDMA transmission with multiple transmit antennas.

SC-FDMA can be found in the literature under different names. It was first conceived in a time-domain implementation [8] called IFDMA (Interleaved Frequency Division Multiple Access), which structurally imposes a distributed subcarrier allocation. At time (t), blocks of M data symbols $x_k^{(t)}, k = 0...M-1$ (*e.g.*, Quaternary Amplitude Modulation (QAM) symbols) are parsed into data blocks $\mathbf{x}^{(t)} = \left[x_0^{(t)}, x_1^{(t)}, ..., x_{M-1}^{(t)}\right]^{\mathrm{T}}$ of duration $T = MT_s$, where T_s is the QAM symbol duration. These blocks are K-time compressed and K-time replicated to form the IFDMA signal with the same duration $T = NT_c$ where $N = KM$ and $T_s = KT_c$, T_c being the chip duration. As theoretically proven in [9], this manipulation has a direct interpretation in the frequency domain: The spectrum of the compressed and K-times replicated signal has the same shape as the original signal, with the difference that it includes exactly $K-1$ zeros between two data subcarriers.

The spectral considerations above open the way to a frequency-domain implementation of SC-FDMA [5], sometimes called DFT-spread OFDM, since precoding is done by means of a DFT. The system model for single antenna SC-FDMA transmission (detailed in [10]) follows a classical structure of precoded-OFDMA system which consists of DFT precoding, zero insertion and subcarrier mapping, followed by IDFT processing and cyclic prefix (CP) insertion. The insertion of space-time (ST) or space-frequency (SF) precoding in a SC-FDMA transmitter must be carefully chosen. It is well known that in OFDMA-like systems, the IDFT operation is equivalent to splitting the information transmitted through a wideband channel into parallel data streams, each one being transmitted by modulating a distinct subcarrier [1], [2]. Thus, ST/SF precoding relying on codes originally designed for the narrowband case should be inserted after DFT precoding at subcarrier level.

Fig. 1 shows how ST/SF precoding can be implemented in a SC-FDMA transmitter with N_{Tx} transmit antennas and M out of N allocated subcarriers. Data block $\mathbf{x}^{(t)}$ consisting in M modulation symbols is DFT-precoded by means of an M-sized DFT $\mathbf{F}_M$, resulting in M-sized vectors $\mathbf{s}^{(t)} = \mathbf{F}_M\mathbf{x}^{(t)}$. From the DFT output, ST/SF precoding generates N_{Tx} vectors $\mathbf{s}^{\mathrm{Tx}_j,(t)}$, $j = 0 \ldots N_{\mathrm{Tx}}-1$, to be mapped following a specific subcarrier allocation described by an $N \times M$ matrix $\mathbf{Q}$ ($N \geq M$) as, *e.g.*:

$$\mathbf{Q}_{N\times M}^{\mathrm{localized}} = \left.\begin{pmatrix} \mathbf{0}_{q\times M} \\ \mathbf{I}_M \\ \mathbf{0}_{(N-q-M)\times M} \end{pmatrix}\right|_{q\in\{0...N-M\}}, \text{ or}$$
$$\mathbf{Q}_{N\times M}^{\mathrm{distributed}} = \mathbf{I}_M \otimes \left.\begin{pmatrix} \mathbf{0}_{n\times 1} \\ 1 \\ \mathbf{0}_{(N/M-n-1)\times 1} \end{pmatrix}\right|_{n\in\{0...M-1\}}, \tag{4}$$

and passed through an *N*-point IDFT. In a vector form, the SC-FDMA symbols generated on each antenna branch become:

$$\mathbf{y}^{\mathrm{Tx}_j,(t)} = \mathbf{F}_N^{-1}\mathbf{Q}\mathbf{s}^{\mathrm{Tx}_j,(t)}. \tag{5}$$

The form of the matrix $\mathbf{Q}$ might lead to contiguous [5], distributed [8], mixed [9] or even channel-dependent subcarrier allocation. We will consider here the contiguous (localized) and the distributed cases, since other schemes may lead to PAPR degradation. In a distributed subcarrier allocation scenario, frequency-domain generated SC-FDMA is strictly identical to time-domain generated IFDMA. To simplify channel estimation, LTE preferred localized subcarrier allocation. A cyclic prefix is usually inserted before transmission (and removed at the receiver before demodulation) to eliminate the

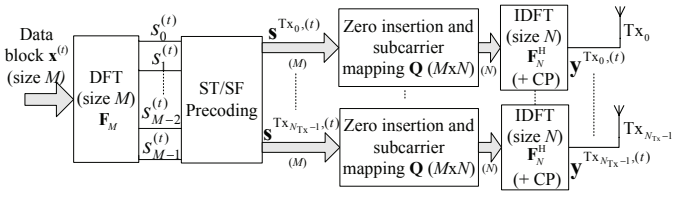

Fig. 1. Block diagram of a SC-FDMA transmitter with ST/SF precoding (M out of N allocated subcarriers, N_{Tx} transmit antennas).

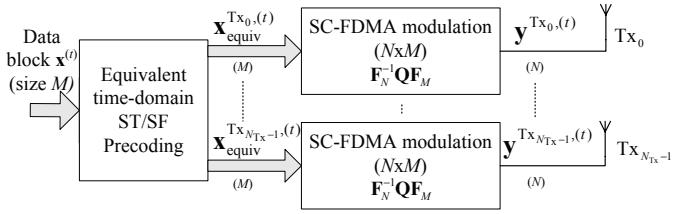

Fig. 2. Block diagram of a SC-FDMA transmitter with time-domain equivalent ST/SF precoding.

inter-symbol interference (ISI) arising from multipath propagation. Here, we will assume that the CP is long enough to absorb the ISI and we will omit it from further representations.

Any frequency manipulation performed in the ST/SF precoding block can be easily translated into the time domain. For any transmit antenna $\mathrm{Tx_j}$, $j = 0...N_{\mathrm{Tx}}-1$, we denote by:

$$\mathbf{x}_{\mathrm{equiv}}^{\mathrm{Tx}_j,(t)} = \mathbf{F}_M^{-1}\mathbf{s}^{\mathrm{Tx}_j,(t)} \tag{6}$$

the equivalent time-domain virtual constellation (dependent on the original constellation $\mathbf{x}(t)$) that would produce $\mathbf{y}^{\mathrm{Tx}_j,(t)}$ when undergoing SC-FDMA modulation, that is:

$$\mathbf{y}^{\mathrm{Tx}_j,(t)} = \mathbf{F}_N^{-1}\mathbf{Q}\mathbf{F}_M\mathbf{x}_{\mathrm{equiv}}^{\mathrm{Tx}_j,(t)}. \tag{7}$$

This interpretation leads to the equivalent transmitter representation in Fig. 2. This model is generally not targeted for a practical implementation of an ST/SF frequency-domain precoded SC-FDMA due to its higher complexity with respect to the one in Fig. 1. We will simply make use of it to give some insight on the signal structure and explain the PAPR properties. This equivalent representation also provides a powerful means to convert the ST/SF precoding family presented in this paper to systems where we have no physical access to the subcarriers (*e.g.*, IFDMA with time-domain implementation).

To describe ST/SF codes, we will first describe the ST/SF precoding matrix and the signal representation in the frequency domain $\mathbf{s}^{\mathrm{Tx}_{0,1},(t)}$. Then, we will describe the equivalent constellations $\mathbf{x}_{\mathrm{equiv}}^{\mathrm{Tx}_{0,1},(t)}$ to be sent to each antenna after SC-FDMA modulation, and finally we will comment on the PAPR properties of SC-FDMA signals based on these constellations.

B. Space-Time Block Codes for SC-FDMA

According to the propagation conditions of each terminal, coding, modulation and MIMO techniques need to be dynamically and jointly optimized to maximize overall network performance. A terminal with good propagation conditions, for example, may enhance its throughput by employing spatial multiplexing techniques, or employ adaptive transmission as a function of the available channel state information (CSI). On the other hand, for a terminal subjected to bad propagation conditions or unreliable CSI (*e.g.*, close to the cell edge or in high velocity scenarios), the best option is to take advantage from transmit diversity. One of the most elegant, simple and well-known transmit diversity schemes for $N_{\mathrm{Tx}} = 2$ transmit antennas was introduced by Alamouti [11]. It is an orthogonal code ensuring full diversity at a rate of one symbol per channel use (half of the maximum achievable data rate), while keeping a very simple optimum decoder. Let us consider the original precoding matrix $\mathbf{A}_{01}$ [11] and an equivalent version $\mathbf{A}_{01}^{(I)}$:

$$\mathbf{A}_{01} = \begin{pmatrix} a_0 & a_1 \\ -a_1^* & a_0^* \end{pmatrix}, \mathbf{A}_{01}^{(I)} = \begin{pmatrix} a_0 & -a_1^* \\ a_1 & a_0^* \end{pmatrix}. \tag{8}$$

Space-time block codes (STBC) [12] can be considered as an attractive solution for SC-FDMA due to their simplicity and performance. The symbol on the i-th row ($i = 0, 1$) and j-th column ($j = 0, 1$) of the matrices (8) is transmitted on the j-th transmit antenna Tx_j during the i-th time interval t_i. In combination with SC-FDMA, this results in a scheme like in Fig. 1, where $N_{\mathrm{Tx}} = 2$ and the ST/SF precoding is an Alamouti-based STBC. Pairs of M-sized vectors $\mathbf{s}^{(t_0)}$ and $\mathbf{s}^{(t_1)}$ obtained through DFT precoding are Alamouti precoded and the resulting signals go through classical OFDMA modulation, *i.e.*, subcarrier allocation (zero insertion and subcarrier mapping), IDFT and CP insertion. For the Alamouti STBC, we choose any of the matrices in (8) with the convention:

$$a_i = s_k^{(t_i)}, \ (\forall k = 0...M-1, \ i = 0, 1). \tag{9}$$

On each of the M occupied subcarriers, Alamouti precoding is performed between the corresponding frequency samples $s_k^{(t_0=2t)}$ and $s_k^{(t_1=2t+1)}$ belonging to two successive time blocks. This allows the receiver to use a simple STBC decoder. An example of precoding with $\mathbf{A}_{01}^{(I)}$ is given in Table I.

TABLE I
EXAMPLE OF STBC PRECODING WITH $\mathbf{A}_{01}^{(I)}$

		Time $t_0 = 2t$	Time $t_1 = 2t+1$
On k-th subcarrier	Tx_0	$s_k^{\mathrm{Tx}_0,(t_0)} = s_k^{(t_0)}$	$s_k^{\mathrm{Tx}_0,(t_1)} = s_k^{(t_1)}$
	Tx_1	$s_k^{\mathrm{Tx}_1,(t_0)} = -\left(s_k^{(t_1)}\right)^*$	$s_k^{\mathrm{Tx}_1,(t_1)} = \left(s_k^{(t_0)}\right)^*$
At block level	Tx_0	$\mathbf{s}^{\mathrm{Tx}_0,(t_0)} = \mathbf{s}^{(t_0)}$	$\mathbf{s}^{\mathrm{Tx}_0,(t_1)} = \mathbf{s}^{(t_1)}$
	Tx_1	$\mathbf{s}^{\mathrm{Tx}_1,(t_0)} = -\left(\mathbf{s}^{(t_1)}\right)^*$	$\mathbf{s}^{\mathrm{Tx}_1,(t_1)} = \left(\mathbf{s}^{(t_0)}\right)^*$

Let us revisit the representation given in Fig. 2. We always send on the first transmit antenna Tx_0 an SC-FDMA signal corresponding to the original constellation $\mathbf{x}(t)$, *i.e.*, $\mathbf{s}^{\mathrm{Tx}_0,(t)} = \mathbf{s}^{(t)}$. This ensures a low-PAPR SC-FDMA signal on the first antenna, independently of the type of ST/SF precoding. Matrix $\mathbf{A}_{01}^{(I)}$ is therefore privileged. From Table I and (6) we have:

$$\left\{\begin{array}{rcl} \mathbf{x}_{\mathrm{equiv}}^{\mathrm{Tx}_0,(t_i)} & = & \mathbf{x}^{(t_i)}, i = 0, 1 \\ \mathbf{x}_{\mathrm{equiv}}^{\mathrm{Tx}_1,(t_0)} & = & \mathbf{F}_M^{-1} \cdot \left(-\mathbf{s}^{(t_1)}\right)^* = -\mathbf{F}_M^{\mathrm{H}}\mathbf{F}_M^{\mathrm{H}}\left(\mathbf{x}^{(t_1)}\right)^* \\ & = & -\left(\bar{\mathbf{x}}^{(t_1)}\right)^* \\ \mathbf{x}_{\mathrm{equiv}}^{\mathrm{Tx}_1,(t_1)} & = & \mathbf{F}_M^{-1} \cdot \left(\mathbf{s}^{(t_0)}\right)^* = \mathbf{F}_M^{\mathrm{H}}\mathbf{F}_M^{\mathrm{H}}\left(\mathbf{x}^{(t_0)}\right)^* \\ & = & \left(\bar{\mathbf{x}}^{(t_0)}\right)^* \end{array}\right. . \tag{10}$$

If the elements of $\mathbf{x}^{(t_{0,1})}$ belong to a QAM constellation, then their complex conjugate time-reversed versions are also sets of QAM symbols. Thus, on both transmit antennas, we always send SC-FDMA modulated signals corresponding to a QAM constellation. Consequently, these signals have strictly the same PAPR as the original signal. Since STBC precoding is performed for each subcarrier independently, the frequency structure of the signal is not impacted and we can consider that Alamouti precoding is performed at block level, as if we were precoding between $\mathbf{s}^{(t_0)}$ and $\mathbf{s}^{(t_1)}$. As a result, SC-FDMA symbols must be precoded by pairs. From a practical point of view, this imposes that all uplink bursts contain an even number of data blocks, which may be hard or impossible to ensure. This type of restriction also prevents the use of some algorithms relying on the flexibility of the data allocation [13]. As another drawback, STBC is also reported in [14] to be sensitive to high vehicular speeds.

C. Space-Frequency Block Codes for SC-FDMA

The idea of using an STBC in the frequency domain as SFBC is not new, and it has been proven [15] that there is no diversity or capacity loss by applying the Alamouti scheme as SFBC with respect to the case where it is applied as STBC. In order to describe the implementation of an Alamouti-type SFBC, let us consider that the symbols on different rows of any of the matrices (8) no longer correspond to transmission over different intervals of time $t_{0,1}$, but to transmission on different subcarriers $k_{0,1}$:

$$a_i = s_{k_i}^{(t)},\ i = 0, 1,\ \ (\forall)\, t. \tag{11}$$

Alamouti precoding classically involves adjacent frequency samples to be mapped onto contiguous subcarriers, *i.e.*, $k_0 = 2k$ and $k_1 = 2k+1$ in a localized allocation scenario or close subcarriers in a distributed allocation scenario so as to allow simple decoding strategies. In contrast to STBC, SFBC does not require data bursts to be composed of an even number of SC-FDMA symbols. It only requires the number of allocated subcarriers M to be even, which is much easier to achieve in practice.

Table II provides the implementation using matrix $\mathbf{A}_{01}^{(I)}$. When SFBC mapping is performed as described in Table II, we send on Tx_0 a SC-FDMA signal corresponding to the original constellation $\mathbf{x}^{(t)}$, *i.e.*, represented in the frequency domain as $\mathbf{s}^{\mathrm{Tx}_0,(t)} = \mathbf{s}^{(t)}$ after SF precoding. $\mathbf{s}^{\mathrm{Tx}_1,(t)}$ is given by:

$$\begin{aligned}\mathbf{s}^{\mathrm{Tx}_1,(t)} &= \left[-s_1^{(t)*}, s_0^{(t)*}, -s_3^{(t)*}, s_2^{(t)*} \ldots - s_{M-1}^{(t)*}, -s_{M-2}^{(t)*}\right]^{\mathrm{T}} \\ &= \mathbf{P}_M^{(\mathbf{J})} \left(\mathbf{s}^{(t)}\right)^*.\end{aligned} \tag{12}$$

A comparison of implementations using matrices $\mathbf{A}_{01}$ and $\mathbf{A}_{01}^{(I)}$ is given in [16]. Using $\mathbf{A}_{01}$ instead of $\mathbf{A}_{01}^{(I)}$ degrades the PAPR on both transmit antennas by about 1 dB with respect to single antenna transmission. Using $\mathbf{A}_{01}^{(I)}$ turns out to be more convenient, since the signal on Tx_0 is undistorted. The PAPR loss on the second transmit antenna will be evaluated in Section V.

TABLE II
EXAMPLE OF SFBC (RESP. SC-SFBC) PRECODING WITH $\mathbf{A}_{01}^{(I)}$

At time t		Subcarier $k_0 = 2k$	Subcarrier $k_1 = 2k+1$ (resp. $k_1 = 2p-1-k_0$)
At sub-carrier level	Tx_0	$s_{k_0}^{\mathrm{Tx}_0,(t)} = s_{k_0}^{(t)}$	$s_{k_1}^{\mathrm{Tx}_0,(t)} = s_{k_1}^{(t)}$
	Tx_1	$s_{k_0}^{\mathrm{Tx}_1,(t)} = -\left(s_{k_1}^{(t)}\right)^*$	$s_{k_1}^{\mathrm{Tx}_1,(t)} = \left(s_{k_0}^{(t)}\right)^*$
At block level	Tx_0	$\mathbf{s}^{\mathrm{Tx}_0,(t)} = \mathbf{s}^{(t)}$	
	Tx_1	$\mathbf{s}^{\mathrm{Tx}_1,(t)} = \mathbf{P}_M^{(\mathbf{J})} \left(\mathbf{s}^{(t)}\right)^*$ $\left(\mathrm{resp.}\mathbf{s}^{\mathrm{Tx}_1,(t)} = \mathbf{P}_M \left(\mathbf{s}^{(t)}\right)^*\right)$	

In order to understand the impact of SFBC mapping with $\mathbf{A}_{01}^{(I)}$ on the time-domain SC-FDMA signal sent on Tx_1, let us consider the equivalent-constellation representation. Since all operations are performed within the same SC-FDMA symbol, we will omit the superscript (t) in the following. From (6), the equivalent-constellation representation is thus given by:

$$\begin{cases} \mathbf{x}_{\mathrm{equiv}}^{\mathrm{Tx}_0} = \mathbf{x} \\ \mathbf{x}_{\mathrm{equiv}}^{\mathrm{Tx}_1} = \mathbf{F}_M^{-1} \cdot \mathbf{P}_M^{(\mathbf{J})} \mathbf{s}^* = \mathbf{F}_M^{-1} \mathbf{P}_M^{(\mathbf{J})} \mathbf{F}_M^{-1} \cdot \mathbf{x}^* \end{cases}, \tag{13}$$

where $\mathbf{P}_M^{(\mathbf{J})}\mathbf{s}^*$ models the effect of SFBC precoding with matrix $\mathbf{A}_{01}^{(I)}$ on Tx_1 as explained in (12). The (m,n)-th element of matrix $\mathbf{F}_M^{-1}\mathbf{P}_M^{(\mathbf{J})}\mathbf{F}_M^{-1} \triangleq \mathbf{\Pi}^{(\mathbf{J})}$ $(m, n = 0 \ldots M-1)$ can be computed as:

$$\begin{aligned}\Pi_{m,n}^{(\mathbf{J})} &= \sum_{k=0}^{M-1} F_{m,k}^* \left(\sum_{\ell=0}^{M-1} P_{k,\ell}^{(\mathbf{J})} F_{\ell,n}^*\right) \\ &= \tfrac{1}{M} \sum_{k=0}^{M-1} \sum_{\ell=0}^{M-1} P_{k,\ell}^{(\mathbf{J})} \omega_M^{-(km+\ell n)}\end{aligned}. \tag{14}$$

But since $\mathbf{P}_M^{(\mathbf{J})}$ (given in (1)) is a sparse block diagonal matrix containing $M/2$ repetitions of matrix $\mathbf{J}$, we can isolate $M/2$ groups of two non-null elements and rewrite:

$$\begin{aligned}\Pi_{m,n}^{(\mathbf{J})} &= \tfrac{1}{M} \sum_{q=0}^{M/2-1} \left(-\omega_M^{-(2qm+(2q+1)n)} + \omega_M^{-((2q+1)m+2qn)}\right) \\ &= \tfrac{\omega_M^{-m} - \omega_M^{-n}}{M} \sum_{q=0}^{M/2-1} \left(\omega_M^{-2(m+n)}\right)^q \\ &= \begin{cases} \frac{1}{2}(\omega_M^{-m} - \omega_M^{-n}), & \text{if } [2\,(m+n)] \bmod M = 0 \\ 0, & \text{otherwise.} \end{cases}\end{aligned} \tag{15}$$

In conjunction with (13), this gives the elements of the equivalent constellation $\mathbf{x}_{\mathrm{equiv}}^{\mathrm{Tx}_1}$ as a function of the original constellation elements:

$$\begin{aligned}x_{m,\mathrm{equiv}}^{\mathrm{Tx}_1} &= \sum_{n=0}^{M-1} \Pi_{m,n}^{(\mathbf{J})} x_n^* = \sum_{n \in \{M-m, M/2-m\}} \Pi_{m,n}^{(\mathbf{J})} x_n^* \\ &= \cos\left(2\pi \tfrac{m}{M}\right) x_{(M/2-m) \bmod M}^* \\ &\quad + j \sin\left(2\pi \tfrac{m}{M}\right) x_{M-m}^*.\end{aligned} \tag{16}$$

By applying inequality (I1) to relation (16), it can easily be seen that the maximum attainable peak power of the equivalent constellation $\mathbf{x}_{\mathrm{equiv}}^{\mathrm{Tx}_1}$ is doubled with respect to $\mathbf{x}$, since:

$$\begin{aligned}\max\left(\left|\mathbf{x}_{\text{equiv}}^{\text{Tx}_1}\right|^2\right) &= \max_m\left(\left|x_{m,\text{equiv}}^{\text{Tx}_1}\right|^2\right)\\ &\leq \max_m\left(\left|x_{M-m}\right|^2+\left|x_{M/2-m}\right|^2\right)\\ &= 2\max\left(|\mathbf{x}|^2\right).\end{aligned} \tag{17}$$

Equality is attained when $\arg\left(x_{M/2-m}/x_{M-m}\right)=\pi/2$, $m = M/8$. The mean power is not affected, since all operations in (13) preserve the mean power. The PAPR of the equivalent constellation is thus higher on Tx_1, which indicates that the resulting SC-FDMA signal will also have a higher PAPR. If SC-FDMA follows perfectly distributed subcarrier mapping, $\mathbf{y}$ consists of the compression and repetition of samples $\mathbf{x}$. If the maximum peak of the equivalent constellation $\mathbf{x}_{\text{equiv}}^{\text{Tx}_1}$ is doubled with respect to $\mathbf{x}$, so will be the maximum peak of the resulting signal. In localized subcarrier mapping, the SC-FDMA modulation operation $\mathbf{F}_N^{-1}\mathbf{Q}\mathbf{F}_M$ with, *e.g.*, $\mathbf{Q} = [\mathbf{I}_M\ \mathbf{0}_{M\times(N-M)}]^{\text{T}}$, is completely equivalent to an oversampling operation with factor N/M. The signal on Tx_1 can be therefore expected to have a higher PAPR than the signal on Tx_0, since it is the result of oversampling of a signal with higher dynamic range. Numerical simulations evaluating the PAPR of SFBC will be presented in Section V.

III. Orthogonal Single-Carrier SFBC for Two Transmit Antennas

In the previous section, we have shown that the use of STBC is limited to data bursts composed of an even number of SC-FDMA symbols and that classical SFBC performs frequency shuffling $\mathbf{P}_M^{(\mathbf{J})}$ which results in increasing the PAPR of the equivalent constellation $\mathbf{x}_{\text{equiv}}^{\text{Tx}_1}$, and thus of the resulting SC-FDMA signal transmitted on Tx_1. Our purpose here is to design a modified SFBC where we replace $\mathbf{P}_M^{(\mathbf{J})}$ by a matrix $\mathbf{P}_M$ such that $\mathbf{x}_{\text{equiv}}^{\text{Tx}_1} = \mathbf{F}_M^{-1}\mathbf{P}_M\mathbf{F}_M^{-1}\cdot\mathbf{x}^* \triangleq \mathbf{\Pi}\mathbf{x}^*$ has good PAPR properties. We will proceed as follows:

- Find a matrix $\mathbf{P}_M$ corresponding to an Alamouti-type SFBC operation such that the PAPR of the equivalent constellation $\mathbf{x}_{\text{equiv}}^{\text{Tx}_1}$ is the same as the PAPR of the original constellation $\mathbf{x}$;
- Interpret the impact of the Alamouti-type SFBC operation $\mathbf{s}^{\text{Tx}_1} = \mathbf{P}_M\mathbf{s}^{\text{Tx}_0*}$ onto the time-domain equivalent constellation $\mathbf{x}_{\text{equiv}}^{\text{Tx}_1}$ and onto the frequency samples $\mathbf{s}^{\text{Tx}_1}$, and prove that the operation $\mathbf{P}_M$ leads to signals $\mathbf{y}^{\text{Tx}_{0,1}}$ exhibiting the same PAPR on both transmit antennas.

We are searching a matrix $\mathbf{P}_M$ such as $\mathbf{x}_{\text{equiv}}^{\text{Tx}_1}$ has the same amplitude distribution as $\mathbf{x}$, *i.e.*, the following three sets have the same elements:

$$\begin{aligned}\left\{\left|x_{m,\text{equiv}}^{\text{Tx}_1}\right|_{m=0\ldots M-1}\right\} &= \left\{\left|x_{m,\text{equiv}}^{\text{Tx}_0}\right|_{m=0\ldots M-1}\right\}\\ &= \left\{|x_m|_{m=0\ldots M-1}\right\}.\end{aligned} \tag{18}$$

This condition ensures that the PAPRs of $\mathbf{y}^{\text{Tx}_{0,1}}$ have the same upper bound. It is proven in Appendix A that:

$$\mathbf{P}_M = -\mathbf{S}_M^{2p}\bar{\mathbf{P}}_M^{(\mathbf{J})}, \tag{19}$$

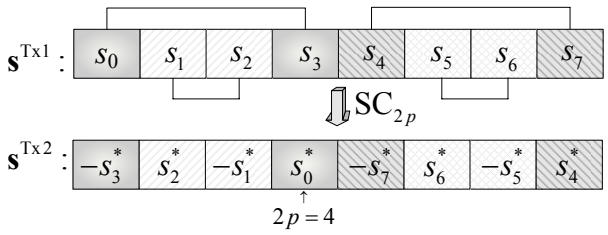

Fig. 3. SC-SFBC precoding; example for $M = 8$, $2p = 4$.

where p is an integer parameter, corresponds to an Alamouti-type operation in the frequency domain satisfying (18). At sample level in the frequency domain, this gives:

$$s_k^{\text{Tx}_1} = (-1)^{k+1}s^*_{(2p-1-k)\bmod M}, (k = 0\ldots M-1). \tag{20}$$

We will call this space-frequency precoding "single-carrier SFBC" (SC-SFBC). In the sequel, we will denote by SC_{2p} the operation transforming $\mathbf{s}^{\text{Tx}_0} = \mathbf{s}$ into:

$$\mathbf{s}^{\text{Tx}_1} = \mathbf{P}_M\mathbf{s}^* \triangleq \text{SC}_{2p}(\mathbf{s}). \tag{21}$$

The SC_{2p} operation takes the complex conjugates of a vector $\mathbf{s}$ in reversed order, applies alternative sign changes and then cyclically shifts down its elements by $2p$ positions. This is depicted in Fig. 3. Alamouti-precoded pairs appear onto non-adjacent frequency samples $(k_0, k_1 = \text{f}(k_0))$, with k_0 even and:

$$\text{f}(k) = (2p-1-k)\bmod M. \tag{22}$$

Indeed, for the example presented in Fig. 3, Alamouti precoding with matrix $\mathbf{A}_{01}^{(I)}$ is performed between the following pairs (k_0, k_1) of frequency samples: (0,3), (2,1), (4,7), (6,5). Eq. (11) still stands, but k_0 and k_1 are no longer consecutive. Table II summarizes the differences between classical SFBC and SC-SFBC precoding operations in the frequency domain.

Let us now investigate the properties of the equivalent constellation generated by SC-SFBC precoding. $\mathbf{x}_{\text{equiv}}^{\text{Tx}_1}$ is determined by applying IDFT transform to (20):

$$\begin{aligned}x_{m,\text{equiv}}^{\text{Tx}_1} &= \tfrac{1}{\sqrt{M}}\sum_{k=0}^{M-1}s_k^{\text{Tx}_1}\omega_M^{-km}\\ &= \tfrac{1}{\sqrt{M}}\sum_{k=0}^{M-1}\underbrace{(-1)^{k+1}}_{\omega_M^{M/2(k+1)}}s^*_{(2p-1-k)\bmod M}\omega_M^{-km}\\ &= \tfrac{1}{\sqrt{M}}\sum_{k=0}^{M-1}s_k^*\omega_M^{-(2p-1)m+k(m+M/2)}\\ &= \omega_M^{-(2p-1)m}x^*_{(m+M/2)\bmod M}.\end{aligned} \tag{23}$$

Equivalent constellation $\mathbf{x}_{\text{equiv}}^{\text{Tx}_1}$ is obtained via complex conjugation and phase shifts applied to the original constellation points, but no amplitude modification is performed: Design criterion (18) is obviously satisfied. Let us assume that $\mathbf{x}$ is composed of Quaternary Phase-Shift Keying (QPSK) symbols, for example. In this case, antenna Tx_1 transmits an SC-FDMA signal based on a M'-PSK constellation where $M' = \gcd(M, 2p-1)$ (we have denoted by $\gcd(a,b)$ the

greatest common divisor of the integers a and b). Let us now analyze how SC-SFBC and the constellation rotation introduced by it impact the PAPR of the transmitted signals. In the case of perfectly distributed subcarrier allocation, where $\mathbf{y}^{\mathrm{Tx}_{0,1}}$ appears as the repetition of contracted $\mathbf{x}^{\mathrm{Tx}_{0,1}}_{\mathrm{equiv}}$ sequence, by expressing any $n = 0...N-1$ with respect to its integer quotient k and remainder r with respect to division by M, we can state:

$$\begin{aligned}\left|y^{\mathrm{Tx}_1}_{n=km+r}\right| &= \left|x^{\mathrm{Tx}_1}_{r,\mathrm{equiv}}\right| = \left|\omega_M^{-(2p-1)m} x^*_{(r+M/2) \bmod M}\right| \\ &= \left|x_{(r+M/2) \bmod M}\right| = \left|y^{\mathrm{Tx}_0}_{km+(r+M/2) \bmod M}\right|.\end{aligned} \tag{24}$$

If the system follows localized subcarrier allocation with, *e.g.*, $\mathbf{Q} = \left[\begin{array}{cc} \mathbf{I}_M & \mathbf{0}_{M\times(N-M)} \end{array}\right]^{\mathrm{T}}$, we obtain:

$$\begin{aligned}\left|y^{\mathrm{Tx}_1}_n\right| &= \left|\frac{1}{\sqrt{N}} \sum_{k=0}^{M-1} (-1)^k s^*_{\underbrace{(2p-1-k) \bmod M}_{\to \ell}} \omega_N^{-kn}\right| \\ &= \left|\frac{1}{\sqrt{N}} \sum_{\ell=0}^{M-1} \omega_N^{-(2p-1)n} \underbrace{(-1)^\ell}_{\omega_N^{\ell N/2}} s^*_\ell \omega_N^{\ell n}\right| \\ &= \left|\left(\frac{1}{\sqrt{N}} \sum_{\ell=0}^{M-1} s_\ell \omega_N^{-\ell(n+N/2)}\right)^*\right| \\ &= \left|y^{\mathrm{Tx}_0 *}_{n+N/2}\right| = \left|y^{\mathrm{Tx}_0}_{n+N/2}\right|.\end{aligned} \tag{25}$$

In amplitude, the samples to be sent on Tx_1 are a reordering of the samples to be sent on Tx_0. $\mathbf{y}^{\mathrm{Tx}_{0,1}}$ have strictly the same amplitude distribution and therefore strictly the same PAPR. We will say that SC_{2p} is an *SC-orthogonal* operation, *i.e.*, orthogonal and not causing any PAPR variation.

However, as a consequence of keeping the good PAPR properties, SC-SFBC jointly encodes samples which may be allocated to distant subcarriers. Specifically, precoding is performed between non-adjacent samples k_0 and $k_1 = (2p-1-k_0) \bmod M$. Thus, these samples might experience rather different channel realizations and we can expect some performance degradation with respect to conventional SFBC. To minimize this degradation, we minimize the maximum distance between frequency samples involved in the SC-SFBC precoding by choosing $2p$ as close as possible to $M/2$.

IV. Quasi-Orthogonal SC-SFBC for Four Transmit Antennas

It was proven [17] that complex orthogonal designs of rate one symbol per channel use do not exist for more than two transmit antennas. Therefore, in order to keep rate one symbol per channel use, we have to relax the orthogonality condition and search for Quasi-Orthogonal (QO) codes that are compatible with the SC-FDMA signal structure. Let us investigate the Alamouti-extended codes introduced by Jafarkhani [18] for systems with 4 transmit antennas. Employing such a code in the time-dimension (QOSTBC) implies coding between symbols on the same k-th subcarrier but coming from 4 time-consecutive data blocks (e.g., $s_k^{(4t)} s_k^{(4t+1)} s_k^{(4t+2)} s_k^{(4t+3)}$). This assumes that all uplink bursts contain a multiple of 4 SC-FDMA symbols, which is difficult to meet in practice. Alternatively, if we use such a code in the frequency-dimension as classical QOSFBC (*i.e.*, precoding is applied within the same SC-FDMA symbol among 4 adjacent frequency samples $s_{4k} s_{4k+1} s_{4k+2} s_{4k+3}$), the frequency permutations involved break the low-PAPR property of the signal and cause an important PAPR degradation.

To preserve the framing compatibility of SF-type precoding without causing any PAPR degradation, let us extend the SC-SFBC precoding principle to the case of four transmit antennas. First, in order to obtain a QO code, we need to satisfy the following QO condition: For each $\mathbf{s}^{\mathrm{Tx}_i}$, $i = 0...3$, two out of the three precoded vectors $\mathbf{s}^{\mathrm{Tx}_j}$, $(j = 0...3, j \neq i$ should be obtained via an orthogonal operation applied to $\mathbf{s}^{\mathrm{Tx}_i}$. Furthermore, in order not to degrade the PAPR, this orthogonal operation must be PAPR-invariant. Since the SC_{2p} operation defined in (21) is both orthogonal and PAPR-invariant, we will impose the following condition: For each $\mathbf{s}^{\mathrm{Tx}_i}$, two out of the three precoded vectors $\mathbf{s}^{\mathrm{Tx}_j}$, $(j \neq i; i, j = 0...3)$ should be SC-orthogonal to $\mathbf{s}^{\mathrm{Tx}_i}$, *e.g.*, $\mathbf{s}^{\mathrm{Tx}_0}$ and $\mathbf{s}^{\mathrm{Tx}_2}$ are both SC-orthogonal to $\mathbf{s}^{\mathrm{Tx}_1}$ and to $\mathbf{s}^{\mathrm{Tx}_3}$, which gives:

$$\left\{\begin{array}{l} \mathbf{s}^{\mathrm{Tx}_1} = \mathrm{SC}_{2p}(\mathbf{s}^{\mathrm{Tx}_0}) = \mathrm{SC}_{2p'}(\mathbf{s}^{\mathrm{Tx}_2}) \\ \mathbf{s}^{\mathrm{Tx}_3} = \mathrm{SC}_{2p''}(\mathbf{s}^{\mathrm{Tx}_0}) = \mathrm{SC}_{2p'''}(\mathbf{s}^{\mathrm{Tx}_2}) \end{array}\right. . \tag{26}$$

It is proven in Appendix B that this leads to $p' = p'' = p - M/4$ and $p''' = p$. This results in precoding between non-adjacent frequency samples $s_{k_{0\ldots3}}$, where $k_{0\ldots3}$ are given below. Index k_0 can be restricted to even values less than $M/2$ so that (k_0, k_1, k_2, k_3) sweeps the range $0...M-1$ without index superposition:

$$\left\{\begin{array}{l} k_1 = (2p-1-k_0) \bmod M \\ k_2 = (k_0 - M/2) \bmod M \\ k_3 = (2p - M/2 - 1 - k_0) \bmod M \end{array}\right. , \; k_0 < \frac{M}{2}, \text{ even}. \tag{27}$$

Thus, by its own construction, this Single-Carrier QOSFBC (denoted in the sequel by SC-QOSFBC) ensures SC-like PAPR onto all transmit antennas. The solution is illustrated in Fig. 4. Note that by trying to extend the Alamouti-based code described in Section III, we created a code based on one of the Jafarkhani constructions given in [18] whose components are mapped onto distant subcarriers. Indeed, SF precoding is performed by choosing $a_i = s_{k_i}, i = 0...3$ with k_0 even and inferior to $M/2$, in:

$$\mathbf{A}^{(I)} = \begin{array}{c} \left(\begin{array}{cccc} a_0 & -a_1^* & a_2 & -a_3^* \\ a_1 & a_0^* & a_3 & a_2^* \\ a_2 & -a_3^* & a_0 & -a_1^* \\ a_3 & a_2^* & a_1 & a_0^* \end{array}\right) \\ \begin{array}{cccc} \uparrow & \uparrow & \uparrow & \uparrow \\ \mathrm{Tx}_0 & \mathrm{Tx}_1 & \mathrm{Tx}_2 & \mathrm{Tx}_3 \end{array} \end{array} \begin{array}{l} \leftarrow f_{k_0} \\ \leftarrow f_{k_1} \\ \leftarrow f_{k_2} \\ \leftarrow f_{k_3} \end{array} . \tag{28}$$

The properties of the QO codes (28) were thoroughly investigated in [19]- [20]. We would consequently expect SC-QOSFBC to have similar performance, with a small penalty

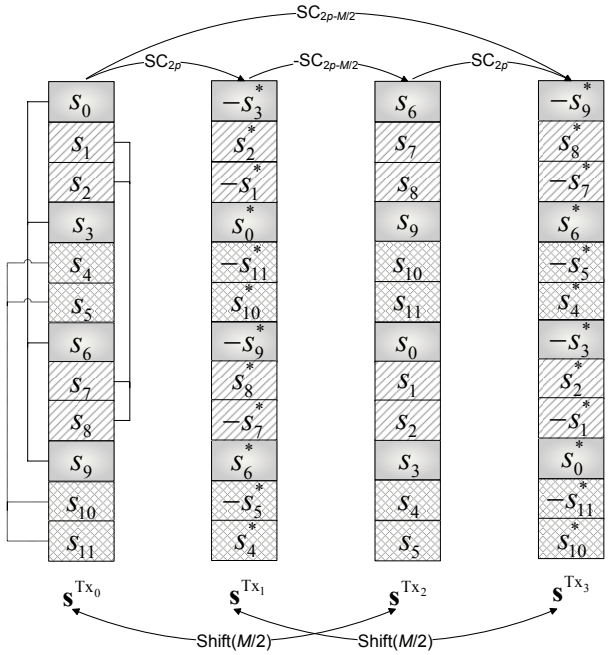

Fig. 4. SC-QOSFBC precoding, example for $M = 12$, $2p = 4$; $(k_0, k_1, k_2, k_3) = \{(0, 3, 6, 9), (2, 1, 8, 7), (4, 11, 10, 5)\}$.

with respect to conventional QOSFBC, which is due to precoding samples to be transmitted onto non-adjacent subcarriers.

V. Simulation Results

We consider a SC-FDMA system with $N = 512$ subcarriers, among which 300 are active data carriers, to fit a bandwidth of 5 MHz. To retrieve frequency diversity, groups of 12 SC-FDMA symbols with QPSK signal mapping are encoded together with a rate-1/2 turbo code using the LTE interleaving pattern [21]. A cyclic prefix with a length of 31 samples is employed. We consider an uncorrelated Vehicular A 3GPP MIMO channel [22] with 6 taps and a maximum delay spread of 2.51 μs. 60 localized subcarriers are allocated to the same user and two or four receive antennas are present at the base station.

Note that Alamouti-based codes were introduced for narrowband transmission with the assumption that the channel does not vary between the two transmission periods. Obviously, using these codes in the frequency domain causes some degradation, because the channel frequency response slightly varies from one subcarrier to another. On the other hand, STBCs suffer from some degradation in the case of high mobility users due to variations of the channel from one symbol to the next. A good strategy in both cases is to minimize the degradation by using an MMSE (Minimum Mean Square Error) receiver instead of the MRC (Maximum Ratio Combining) proposed by Alamouti. MMSE decoding preserves the diversity order at the expense of some noise enhancement [19]. In the simulations, we assume either perfect channel knowledge, or real channel estimation. In this latter case, the frame is composed of 2 slots, each slot being composed of 6 SC-FDMA data symbols split in the middle by one Zadoff-Chu pilot symbol. Channel estimation is performed by frequency smoothing with an 11-tap Wiener filter, followed by time-domain interpolation. Note that in order to allow performance comparison, we used a frame in which the number of SC-FDMA blocks is a multiple of 4 so that it is compatible with both STBC and QOSTBC.

Let us define the Complementary Cumulative Distribution Function (CCDF) of the Instantaneous Normalized Power (INP) of a sequence of digital samples $\mathbf{y}$:

$$\mathrm{CCDF}_{(\mathrm{INP}(\mathbf{y}))}(\gamma^2) = \Pr\left(\frac{|y_i|^2}{E\left\{|\mathbf{y}|^2\right\}} > \gamma^2\right). \qquad (29)$$

This function gives the probability that the INP of a sample y_i exceeds a certain clipping level γ^2. The CCDF of INP takes into account all the samples of the signal and gives a more accurate measurement of the influence of nonlinearity than the largely employed CCDF of PAPR, which considers only the largest peak of each block of samples [23]. In order to correctly evaluate the INP of the transmitted signal, we applied an oversampling factor of 4, which is reported in the literature to be sufficient for an accurate signal description after the nonlinearity [3].

Fig. 5 depicts the CCDF of INP of all the investigated schemes for every transmit antenna. It also includes the CCDF of INP of an equivalent OFDMA transmission, *i.e.*, without DFT precoding as a reference. For all precoding types, we send the original SC-FDMA signal on the transmit antenna Tx_0. As expected, we can see that the proposed SC-SFBC and SC-QOSFBC have very good PAPR performance and preserve the SC nature of the SC-FDMA signal, just as STBC and QOSTBC. On the other hand, as explained in section III, the frequency manipulations involved by SFBC/QOSFBC lead to an increased PAPR. The obtained waveform is a hybrid signal with a PAPR higher than in SC-FDMA but lower than in OFDMA. The amount of degradation depends on the considered transmit antenna because of the different spectrum manipulations involved. At a clipping probability of 10^{-4} for example, we can lose up to 0.9 dB (resp. 1.3 dB) with classical SFBC (resp. QOSFBC) with respect to a PAPR-invariant precoding scheme. Note also by analyzing 28 and Table II that we send the same signal on Tx_1 when using classical QOSFBC and SFBC, and the same PAPR performance is achieved on Tx_1. The advantage of our SC-SFBC and SC-QOSFBC schemes illustrated in Fig. 5 is directly related to the gain in terms of the amplifier back-off. Note that the amplifier back-off in practical systems is often dictated by the spectral mask rather than by in-band distortion, which results from clipping. With the back-off needed to meet the spectral mask requirements, in-band distortion is essentially zero in coded systems and the SNR degradation is reduced to the amplifier back-off. Consequently, the gain illustrated in Fig. 5 is the SNR gain our proposed schemes will achieve over conventional SFBC in the presence of a nonlinear power amplifier due to their reduced PAPR.

Fig. 6 compares the performance of Alamouti-based transmit diversity schemes in terms of Frame Error Rate (FER) for the case of two transmit antennas. SFBC has similar performance as STBC, since there is no significant channel variation

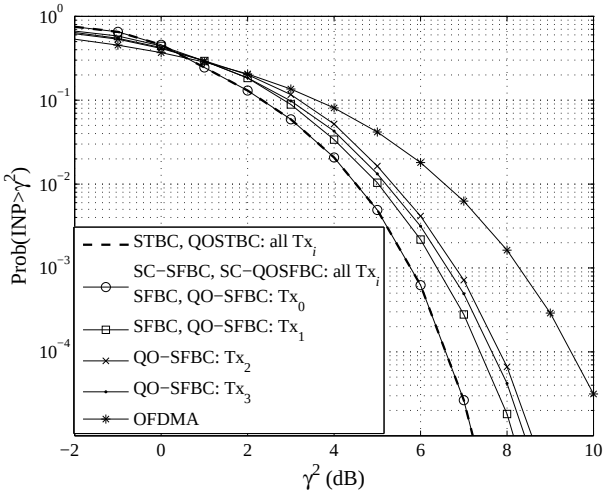

Fig. 5. CCDF of INP, QPSK transmission, $N_{\mathrm{Tx}} = 2/4$ transmit antennas.

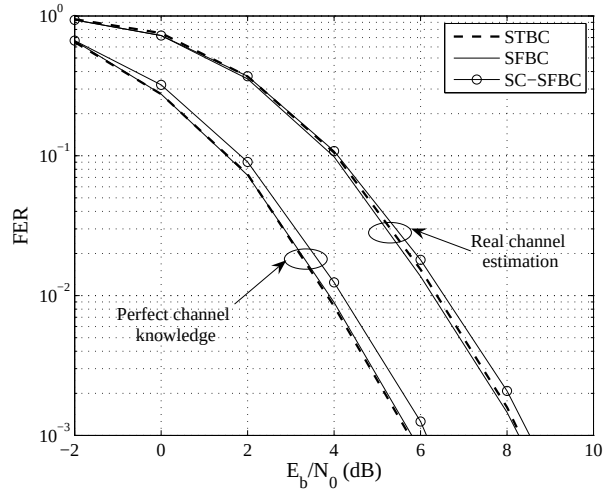

Fig. 6. The influence of channel estimation: 3 km/h, 60 localized subcarriers, QPSK 1/2, MMSE decoding, 2 transmit antennas and 2 receive antennas.

between two adjacent subcarriers. Compared to SFBC, SC-SFBC has a performance loss on the order of 0.3 dB at a target FER of 1%, due to Alamouti precoding between non-adjacent frequency samples. But since SFBC loses up to 0.9 dB in terms of PAPR with respect to SC-SFBC or STBC, we can conclude that SC-SFBC has better overall performance than classical SFBC. The same relative behavior is reported for any vehicular speed. Employing actual channel estimation causes a loss for all schemes around 2.4 dB, due to the estimation errors and to the energy spent by pilots. Note however that with channel estimation errors, the additional degradation brought by SC-SFBC is slightly masked and thus reduced as compared to SFBC and STBC (0.15 dB).

In Fig. 7 we analyze the system performance at high vehicular speeds (120 km/h) with real channel estimation. STBC, which is more sensitive to Doppler shifts than the SFBC-based techniques, is outperformed by SFBC (0.2 dB) and exhibits similar performance to SC-SFBC. Since SC-SFBC benefits

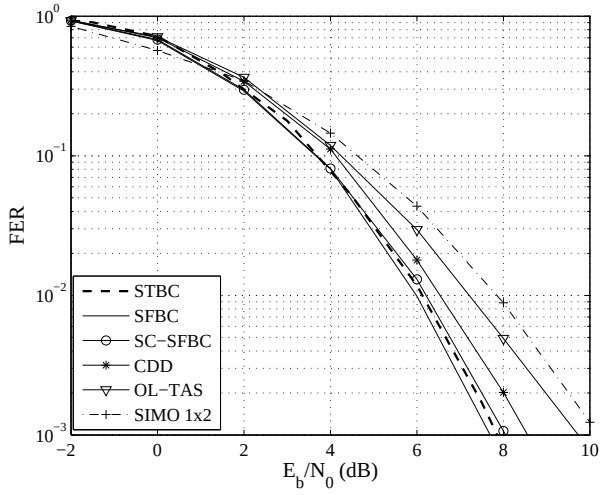

Fig. 7. Comparison with other open-loop diversity schemes: 120 km/h, 60 localized subcarriers, QPSK 1/2, MMSE decoding with real channel estimation, 2 transmit antennas and 2 receive antennas.

from the advantages of both SFBC (high flexibility, robustness at high vehicular speeds) and STBC (low PAPR), we conclude that it is a very suitable technique when combined with SC-FDMA. Results in [24], [25] presenting the performance of such a system with conventional MRC and/or small number of distributed subcarriers lead to the same conclusions. We also compare here these two techniques with other simple well-known transmit diversity techniques. CDD (Cyclic Delay Diversity) [26] consists in splitting the signal after the N-point IDFT between the two antenna branches: The original SC-FDMA symbol is sent on Tx_0, and the symbol on Tx_1 is cyclically shifted by a delay δ. This transforms a system with multiple transmit antennas into an equivalent single transmit antenna system. The transformed channel finds its frequency selectivity increased as a result of the virtual echoes produced by the CDD technique. We use here a CDD with $\delta = 128$ samples. In Open-Loop Transmit Antenna Selection (OL-TAS), diversity is achieved by switching between multiple transmit antennas during the transmission of a coded data frame, in the absence of channel state information at the transmitter. With two transmit antennas, OL-TAS only needs a single RF chain but is more vulnerable to high vehicular speeds than its other counterparts: Because of the antenna switching, each pilot will be used to estimate the channel onto one slot, and no time interpolation can consequently be employed between both slots of the same frame. Even if all transmit diversity techniques show performance improvements compared to single antenna transmission (referred to as Single Input Multiple Output - SIMO 1x2 in the legend), we can see that CDD and OL-TAS are outperformed by the Alamouti-based techniques, by 0.5 dB and 1.2 dB, respectively.

The good behavior of the Alamouti schemes is confirmed by Fig. 8, where performance of a 4-antenna system at 300 km/h with real channel estimation is shown. QOSFBC slightly outperforms QOSTBC by 0.1 dB and SC-QOSFBC by 0.6 dB when 2 Rx antennas are employed, but the potential PAPR gain of SC-QOSFBC over QOSFBC is also higher in the 4-

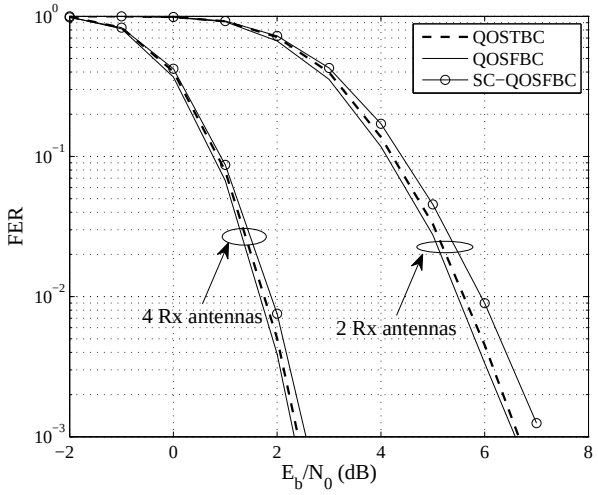

Fig. 8. Four transmit antennas at high vehicular speed: 300 km/h, 60 localized subcarriers, QPSK 1/2, MMSE decoding with real channel estimation, 2/4 receive antennas.

Tx-antenna case. Adding more Rx antennas diminishes the relative loss between SC-QOSFBC and its counterparts.

VI. Conclusion

This paper has analyzed the implementation of Alamouti-based transmit diversity schemes in a SC-FDMA system. We have reviewed the advantages and limitations of existing schemes. First, we have shown that ST codes have implementation-related limitations and that classical SF codes suffer from PAPR degradation when combined with SC-FDMA. Next, we have proposed a family of PAPR-invariant mapping of space-frequency codes suitable for SC-FDMA with two transmit antennas and we derived an extension of this technique to four transmit antennas. This new mapping of Alamouti-based SFBC shows good performance, overall outperforming its classical SFBC counterpart. More flexible than STBC, SC-SFBC and SC-QOSFBC seem to be very suitable solutions to increase the coverage of SC-FDMA systems.

Appendix A

We are searching a matrix $\mathbf{P}_M$ satisfying the design criterion (18). $\mathbf{P}_M$ must be chosen such that an Alamouti-type SFBC correspondence based on matrix $\mathbf{A}_{01}^{(I)}$ exists between the elements of vectors $\mathbf{s}^{\mathrm{Tx}_0}$ and $\mathbf{s}^{\mathrm{Tx}_1} = \mathbf{P}_M \mathbf{s}^{\mathrm{Tx}_0 *}$. $\mathbf{P}_M$ must consequently be a skew symmetric matrix ($\mathbf{P}_M = -\mathbf{P}_M^{\mathrm{T}}$) with only one non-null element per row and per column. Let us denote by $\mathcal{P}$ the class of skew symmetric matrices with elements $p_{m,n}$ $(m,n = 0...M-1)$ in $\{-1,0,1\}$, containing one single non-null element per column and per row in position $(k, \mathrm{f}(k))$. M must be even. Since $\mathbf{P}_M$ has one single non-null element per row and per column, it results that f is a one-to-one transformation of the set $\{0...M-1\}$. If $\mathbf{P}_M \in \mathcal{P}$, then $-\mathbf{P}_M = \mathbf{P}_M^{\mathrm{T}} \in \mathcal{P}$.

Let us define $\mathcal{K}_0$ (resp. $\mathcal{K}_1$) as the $M/2$ sized set of elements k for which $P_{k,\mathrm{f}(k)} = -1$ (resp. 1). Thus, if $k \in \mathcal{K}_0$ then $\mathrm{f}(k) \in \mathcal{K}_1$ because $P_{\mathrm{f}(k),k} = -P_{k,\mathrm{f}(k)} = 1$; also, $\mathrm{f}(\mathrm{f}(k)) = k$ because of the symmetry condition, and it will suffice to define f onto the set $\mathcal{K}_0$. Without loss of generality, we can choose $\mathcal{K}_0$ such as $0 \in \mathcal{K}_0$. From (18) and the properties of $\mathbf{P}_M$, we deduce that $\mathbf{\Pi} = \mathbf{F}_M^{-1}\mathbf{P}_M\mathbf{F}_M^{-1}$ should perform a permutation of the elements in $\mathbf{x}$, possibly accompanied by some phase rotation. $\mathbf{\Pi}$ should consequently belong to the class $\mathit{\Pi}$ of matrices having only one non-null element of type $\mathrm{e}^{j\xi}$ per row and per column, $\xi \in [0, 2\pi)$. $\mathbf{\Pi}$ is also skew symmetric and thus all the elements on its main diagonal are null. We are consequently searching for $\mathbf{P}_M \in \mathcal{P}$ such as $\mathbf{\Pi} = \mathbf{F}_M^{-1}\mathbf{P}_M\mathbf{F}_M^{-1} \in \mathit{\Pi}$. For classical SFBC for example we can easily see from (15) that $\mathbf{F}_M^{-1}\mathbf{P}_M^{(\mathbf{J})}\mathbf{F}_M^{-1}$ is not in $\mathit{\Pi}$ even if $\mathbf{P}_M^{(\mathbf{J})}$ is in $\mathcal{P}$. Let us show that this problem has solutions. We can compute:

$$\begin{aligned}
\Pi_{m,n} &= \sum_{k=0}^{M-1} \tfrac{\omega_M^{-mk}}{\sqrt{M}} \left(\sum_{\ell=0}^{M-1} P_{k,\ell} \tfrac{\omega_M^{-\ell n}}{\sqrt{M}} \right) \\
&= \tfrac{1}{M} \sum_{k=0}^{M-1} \omega_M^{-mk} \left(P_{k,\mathrm{f}(k)} \omega_M^{-n\mathrm{f}(k)} \right) \\
&= \tfrac{1}{M} \sum_{k \in \mathcal{K}_0} \left(P_{k,\mathrm{f}(k)} \omega_M^{-mk-n\mathrm{f}(k)} + P_{\mathrm{f}(k),k} \omega_M^{-m\mathrm{f}(k)-nk} \right) \\
&= \tfrac{1}{M} \sum_{k \in \mathcal{K}_0} \left(-\omega_M^{-(mk+n\mathrm{f}(k))} + \omega_M^{-(m\mathrm{f}(k)+nk)} \right) \\
&= \tfrac{1}{M} \sum_{k \in \mathcal{K}_0} \left(\omega_M^{-(mk+n\mathrm{f}(k)+M/2)} + \omega_M^{-(m\mathrm{f}(k)+nk)} \right), \\
&\quad m,n = 0...M-1.
\end{aligned} \tag{30}$$

Let $\Pi_{0,n_0 \neq 0} = \mathrm{e}^{j\xi_0}$ be the only non-null element on the first row. Since $\Pi_{0,M-n_0} = 1/M \sum_{k \in \mathcal{K}_0} \left(-\omega_M^{-n_0\mathrm{f}(k)} + \omega_M^{-n_0 k} \right) = \Pi_{0,n_0}^* \neq 0$, we deduce $n_0 = (M - n_0) \bmod M$. Since n_0 is not null, $n_0 = M/2$. But $\Pi_{0,M/2} = 1/M \sum_{k \in \mathcal{K}_0} \left[(-1)^k - (-1)^{f(k)} \right] = \mathrm{e}^{j\xi_0}$ is real, thus it can take as values either 1 or -1: either all elements in $\mathcal{K}_0$ are even and all elements in $\mathcal{K}_1 = \mathrm{f}(\mathcal{K}_0)$ are odd, or vice versa. As we have chosen $0 \in \mathcal{K}_0$ by convention, we conclude that $\Pi_{0,M/2} = 1$ and $\mathcal{K}_0 = \{0, 2, \ldots, M-2\}$ contains even integers only. Note that choosing $0 \in K_1$ instead would simply lead to changing the sign of $\mathbf{P}_M$ and trying to find solution $-\mathbf{P}_M$ instead of $\mathbf{P}_M$. Let us apply inequality (I2) to (30). This leads to $|\Pi_{m,n}| \leq 1$. But since $\mathbf{\Pi} \in \mathit{\Pi}$ already implies that $|\Pi_{m,n}| \in \{0,1\}$, we deduce that for all the non-null elements of $\mathbf{\Pi}$ the equality conditions of (I2) must be satisfied and thus all elements in the right-hand part of (30) must have the same argument. For any $m = 0...M-1$, uniquely exists $(\exists!)\, n \neq m$ such that for any k even all elements in the right-hand part of (30) have the same argument (constant with respect to m), let us denote it λ_m. Mathematically, this means:

$$\begin{aligned}
&\forall m, \exists! n \neq m \text{ such that } \forall k \in \mathcal{K}_0, \\
&(mk + n\mathrm{f}(k) + M/2) \bmod M \overset{\lambda_m}{=} (m\mathrm{f}(k) + nk) \bmod M.
\end{aligned} \tag{31}$$

This implies that $[(k - \mathrm{f}(k))(m-n)] \bmod M = M/2$ and thus $(k - \mathrm{f}(k))(m-n) = (2q_k + 1)M/2$, where q_k is an integer depending on k. Let us concentrate on the particular case where M is a power of 2. Given that $k - \mathrm{f}(k)$ is always

odd ($k \in \mathcal{K}_0$ and $\mathrm{f}(k) \in_m athcalK_1$), must equal $M/2$. On each line m the non-null element in $\mathbf{\Pi}$ must be on the column $n = (m + M/2) \bmod M$. Taking $m = 1$ (and implicitly $n = M/2 + 1$) in (31), we find that, for any $k \in \mathcal{K}_0$, $(\mathrm{f}(k) + k + Mk/2) \bmod M \overset{k\text{even}}{=} (\mathrm{f}(k) + k) \bmod M = \lambda_1$. Thus, $k + \mathrm{f}(k)$, independent from m, is a constant odd integer (modulo M) for any k, let it be $\lambda_1 = 2p - 1$ with p integer. We can thus write:

$$\mathrm{f}(k) = (2p - 1 - k) \bmod M, \ \forall k \text{ even}. \tag{32}$$

From (32) we can deduce matrix $\mathbf{P}_M$ with elements -1 in position $(k, \mathrm{f}(k))$ and 1 in position $(\mathrm{f}(k), k)$:

$$\begin{aligned} \mathbf{P}_M &= \begin{bmatrix} \overbrace{\begin{matrix} \mathbf{0}_{2\times 2} & & -\mathbf{J} \\ & \iddots & \\ -\mathbf{J} & & \mathbf{0}_{2\times 2} \end{matrix}}^{2p \text{ elements}} & & \\ & & \mathbf{0}_{2p\times(M-2p)} \\ \mathbf{0}_{(M-2p)\times 2p} & & \\ & \underbrace{\begin{matrix} \mathbf{0}_{2\times 2} & & -\mathbf{J} \\ & \ddots & \\ -\mathbf{J} & & \mathbf{0}_{2\times 2} \end{matrix}}_{M-2p \text{ elements}} & \end{bmatrix} \\ &= -\mathbf{S}_M^{2p} \bar{\mathbf{P}}_M^{(\mathbf{J})}. \end{aligned} \tag{33}$$

With this choice, we can compute the elements of $\mathbf{\Pi}$:

$$\begin{aligned} \Pi_{m,n} &= \tfrac{1}{M} \sum_{k=0}^{M/2-1} \left(\omega_M^{-(2mk+n(2p-1-2k))-M/2} \right. \\ &\quad \left. + \omega_M^{-m(2p-1-2k)-2nk} \right) \\ &= \tfrac{\omega_M^{-n(2p-1)-M/2}}{M} \sum_{k=0}^{M/2-1} \omega_M^{-2(m-n)k} \\ &\quad + \tfrac{\omega_M^{-m(2p-1)}}{M} \sum_{k=0}^{M/2-1} \omega_M^{2(m-n)k}. \end{aligned} \tag{34}$$

Both geometric series here-above sum to $M/2$ when $(2(m-n)) \bmod M = 0$, and to 0 otherwise. Since $\Pi_{m,n} = 0$ for any $m = n$, we can only obtain non-null elements when $(m - n) \bmod M = M/2$, which gives:

$$\Pi_{m,n} = \begin{cases} \omega_M^{-(2p-1)m}, & n = (m + M/2) \bmod M \\ 0, & \text{otherwise.} \end{cases} \tag{35}$$

The design criterion (18) is consequently satisfied and $\mathbf{P}_M = \pm \mathbf{S}_M^p \bar{\mathbf{P}}_M^{(\mathbf{J})}$ leads to a mapping conserving the amplitude distribution of the original constellation. Let us note that (33) verifies the design criterion for any even value of M, since (34) and (35) remain valid when M is not a power of 2. This is not sufficient to state that (33) is the only solution when M is not a power of 2, and other solutions might exist. Nevertheless, in the case $M = 12$ which is typical in LTE, we have verified that no other solutions exist.

APPENDIX B

Let (k_0, k_1, k_2, k_3) be a set of four indices k_i denoting subcarriers encoded together. We concentrate here only on the index of the used frequency samples ($\pm s_{k_0}^{(*)}$ will be represented by k_0). Let us analyze Table III, describing the relationships between the signals sent onto different antennas. To create a valid code, the table must only contain elements from the set (k_0, k_1, k_2, k_3), each element being present once on each line and each column of the table. During the transmission of an arbitrary k_0 on Tx_0, due to the relationships between antennas, k_3 sent on Tx_3 can be expressed in two manners,$k_3 = 2p''' - 2p' + 2p - 1 - k_0$ and $k_3 = 2p'' - 1 - k_0$, which means that $2(p''' - p') = 2(p'' - p)$. During the transmission of k_1 on Tx_0, $2p - 1 - k_1 = k_0$ is sent on Tx_1. On Tx_2 the only choice is to send k_3, which means that $2p' - 1 - k_0 = 2p'' - 1 - k_0$ and thus $2p' = 2p''$. Similarly, we can deduce $2p = 2p'''$. It follows that $2 \cdot 2p = 2 \cdot 2p'$. But $2p$ cannot equal $2p'$ (it would mean that signals on Tx_0 and Tx_2 are equal), and since the equality is written modulo M, $2p = 2p' \pm M/2$.

ACKNOWLEDGMENT

This work was partly supported by the French ANR APOGEE project.

REFERENCES

[1] W. W. R. Forum, Ed., *Technologies for the Wireless Future*. John Wiley & Sons, Ltd, 2006, vol. 2.

[2] H. Sari, G. Karam, and I. Jeanclaude, "Frequency-domain equalization of mobile radio and terrestrial broadcast channels," in *GLOBECOM '94*, Dec. 1994.

[3] J. Tellado, *Multicarrier Modulation with Low Peak to Average Power Applications to xDSL and Broadband Wireless*. Boston/ Dordrecht/ London: Kluwer Academic Publishers, 2000.

[4] Z. Li and X.-G. Xia, "PAPR reduction for repetition space-time-frequency coded MIMO-OFDM systems using Chu sequences," *IEEE Trans. on Wireless Commun.*, vol. 7, no. 4, pp. 1195–1202, Apr. 2008.

[5] "Physical layer aspects for evolved universal terrestrial radio access (UTRA)," 3GPP, Tech. Rep. 25.814 v7.1.0, Sep. 2008.

[6] Z. Wang and G. Giannakis, "Wireless multicarrier communications," *IEEE Signal Processing Mag.*, vol. 17, no. 3, pp. 29–48, May 2000.

[7] G. H. Hardy, J. E. Littlewood, and G. Pólya, *Inequalities*. Cambridge Univ. Press, 1934.

[8] U. Sorger, I. De Broeck, and M. Schnell, "Interleaved FDMA - a new spread-spectrum multiple-access scheme," in *ICC 98*, vol. 2, Jun. 1998, pp. 1013–1017.

[9] T. Frank, A. Klein, and E. Costa, "IFDMA: A scheme combining the advantages of OFDMA and CDMA," *IEEE Trans. on Wireless Commun.*, vol. 14, no. 3, pp. 9–17, Jun. 2007.

[10] C. Ciochina, D. Mottier, and H. Sari, "An analysis of three multiple access techniques for the uplink of future cellular mobile systems," *European Trans. on Telecommunications*, vol. 19, no. 5, pp. 581–588, Jun. 2008.

[11] S. Alamouti, "A simple transmit diversity technique for wireless communications," *IEEE Journal on Sel. Areas in Commun.*, vol. 16, no. 8, pp. 1451–1458, Oct. 1998.

[12] H. Jafarkhani, *Space-Time Coding, Theory and Practice*. Cambridge Univ. Press, 2005.

[13] D. Mottier and L. Brunel, "Idle period shortening for TDD communications in large cells," in *VTC Spring 2006*, May 2006, pp. 72–76.

[14] "Performance evaluations of STBC/SFBC schemes in E-UTRA uplink," Alcatel, 3GPP RAN1 contribution R1-063179.

[15] G. Bauch, "Space-time-frequency transmit diversity in broadband wireless OFDM systems," in *Proc. 8th Intl. OFDM Workshop*, Sep. 2003.

[16] D. Li, P. Lei, and X. Zhu, "Novel space-time coding and mapping scheme in single-carrier FDMA systems," in *PIMRC 2007*, Sep. 2007.

[17] V. Tarokh, H. Jafarkhani, and A. Calderbank, "Space-time block codes from orthogonal designs," *IEEE Trans. on Information Theory*, vol. 45, no. 5, pp. 1456–1467, Jul. 1999.

[18] H. Jafarkhani, "A quasi-orthogonal space-time block code," *IEEE Trans. on Communications*, vol. 49, no. 1, pp. 1–4, Jan. 2001.

[19] M. Rupp and C. Mecklenbräuker, "On extended Alamouti schemes for space-time coding," in *PIMRC 2002*, vol. 1, Oct. 2002, pp. 115–119.

TABLE III
RELATIONSHIPS BETWEEN INDICES IN SC-QOSFBC

	Subcarrier	Tx_0	Tx_1	Tx_2	Tx_3
$\mathrm{Tx}_0 \xrightarrow{\mathrm{SC}_M^p} \mathrm{Tx}_1$; $\mathrm{SC}_M^{p''}$, $\mathrm{SC}_M^{p'}$; $\mathrm{Tx}_3 \xleftarrow{\mathrm{SC}_M^{p'''}} \mathrm{Tx}_2$	f_{k_0}	k_0	$2p-1-k_0$	$2(p'-p)+k_0$	$2(p'''-p'+p)-1-k_0 = 2p''-1-k_0$
	f_{k_1}	$2p-1-k_0$	k_0	$2p'-1-k_0$	$2(p'''-p')+k_0$
	f_{k_2}	$2p'-2p+k_0$	$4p-2p'-1-k_0$	$4(p'-p)+k_0$	$2p'''-4p'+4p-1-k_0$
	f_{k_3}	$2p''-1-k_0$	$2p-2p''+k_0$	$2p'''-1-k_0$	k_0

[20] C. Mecklenbräuker and M. Rupp, "Generalized Alamouti codes for trading quality of service against data rate in MIMO UMTS," *EURASIP Journal on Applied Signal Processing*, no. 5, pp. 662–675, May 2004.

[21] "Evolved universal terrestrial radio access; multiplexing and channel coding," 3GPP, Tech. Rep. 36.212 v8.3.0, May 2008.

[22] "Spatial channel model for MIMO simulations," 3GPP, Tech. Rep. 25.996 v7.0.0, Jun. 2007.

[23] C. Ciochina, F. Buda, and H. Sari, "An analysis of OFDM peak power reduction techniques for WiMAX systems," in *ICC '06*, vol. 10, Jun. 2006, pp. 4676–4681.

[24] C. Ciochina, D. Castelain, D. Mottier, and H. Sari, "A novel space-frequency coding scheme for single carrier modulations," in *PIMRC 2007*, Sep. 2007.

[25] ——, "Single-carrier space-frequency block coding: Performance evaluation," in *VTC Fall 2007*, Oct. 2007, pp. 715–719.

[26] A. Damman and S. Kaiser, "Performance of low complex antenna diversity techniques for mobile OFDM systems," in *Proc. of the MC-SS 2001*, Sep. 2001, pp. 53–64.

Cristina Ciochina was born in Bucharest, Romania, in 1980. She received her engineering degree in electronics and telecommunications from the Polytechnic University of Bucharest, Romania, in 2004. She received her M.Sc. degree from École Supérieure d'Électricité (Supélec), France in 2005 and her Ph.D. degree from Université Paris-Sud XI, France, in 2009, both in telecommunications. Since 2005, she is with Mitsubishi Electric R&D Centre Europe (MERCE), France. Her technical interests include physical layer design, multi-carrier systems, signal processing for future wireless communications systems, 3GPP/LTE. Dr. Ciochina has published 16 technical papers and is the author or co-author of 5 patents.

Damien Castelain was born in Roubaix, France, in 1959. He graduated from the Ecole Nationale Supérieure des Télécommunications (ENST) in 1982. He joined CIT-Alcatel in 1983, where he participated in the development of videophone (COST211) and satellite transmission equipment. He joined France Telecom R&D (CCETT) in 1988, where his main interests were digital broadcasting technologies, multi-carrier systems, channel coding theory and VLSI implementation. From 1988 to 1994, he was involved in Digital Audio Broadcasting (DAB) developments and standardisation. From 1990 to 1998, he was involved in development and standardisation of DVB-T digital terrestrial television. He joined Mitsubishi Electric MERCE in 1998, to coordinate research activities in digital communications applied to wireless systems, mainly Hiperlan/2, 3GPP/UMTS, 3GPP/LTE. He is author or co-author of 30 patents, and has published 33 technical papers.

David Mottier was born in Domfront, France, in 1970. He received the engineering degree in electronics from the Institut National des Sciences Appliquées (INSA), France, in 1993. In 1997, he received the Ph.D. degree in electronics and telecommunications from INSA. His early research was focused on synchronisation, adaptive equalisation and channel decoding for digital video broadcasting systems at France Telecom. He is currently working as head of research of the Communication division and research manager of the Wireless Communication Systems department for the research laboratory Mitsubishi Electric R&D Centre Europe (MERCE) in Rennes, France. His technical interest includes physical layer design, advanced signal processing and network architectures for future wireless and wired communication systems. Dr. Mottier has published 32 papers in international scientific journals and conferences and is the author or co-author of more than 40 patents.

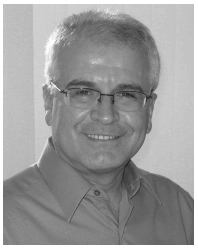

Hikmet Sari (S'78 - M'81 - SM'88 - F'95) received his Diploma (M.S.) and Doctorate in Telecommunications Engineering from the ENST, Paris, France, in 1978 and 1980, respectively, and the Habilitation degree from the University of Paris-Sud, Orsay in 1992. He was with Philips Research Laboratories from 1978 to 1989, first as Researcher and then as Group Supervisor. From 1989 to 1996, he was R&D Department Manager at SAT (SAGEM Group), and from 1996 to 2000, he was Technical Director at Alcatel. In May 2000, he became Chief Scientist of the newly-founded Pacific Broadband Communications, which was acquired by Juniper Networks in December 2001. Since April 2003, he has been a Professor and Head of the Telecommunications Department at SUPELEC, and since December 2004 he is also Chief Scientist of Sequans Communications.

Dr. Sari has published over 180 technical papers and holds over 25 patents. He was an Editor of the IEEE Transactions on Communications from 1987 to 1991, a Guest Editor of the European Transactions on Telecommunications (ETT) in 1993, a Guest Editor of the IEEE JSAC in 1999, an Associate Editor of the IEEE Communications Letters from 1999 to 2002, and a Guest Editor of the EURASIP Journal on Wireless Communications and Networking in 2007. He was also Chair of the Communication Theory Symposium of ICC 2002 (April 2002, New York), Technical Program Chair of ICC 2004 (June 2004, Paris), and Vice General Chair of ICC 2006 (June 2006, Istanbul). He is currently serving as General Chair for the forthcoming PIMRC 2010 and WCNC 2012. He was elevated to the IEEE Fellow Grade and received the Andre Blondel Medal from the SEE (France) in 1995 and he received the Edwin H. Armstrong Achievement Award from the IEEE Communications Society in 2003.